P.O.Box 2345, Beijing 100023,China
Fax: +86-10-85381893
E-mail: wjg@wjgnet.com www.wjgnet.com

World J Gastroenterol 2003;9(10):2317-2321
World Journal of Gastroenterology
 ISSN 1007-9327

• CLINICAL RESEARCH •

Budd-Chiari syndrome: Diagnosis with three-dimensional contrast-enhanced magnetic resonance angiography

Jiang Lin, Xiao-Hai Chen, Kang-Rong Zhou, Zu-Wang Chen, Jian-Hua Wang, Zhi-Ping Yan, Ping Wang

Jiang Lin, Xiao-Hai Chen, Kang-Rong Zhou, Zu-Wang Chen, Jian-Hua Wang, Zhi-Ping Yan, Ping Wang, Department of Radiology, Affiliated Zhongshan Hospital, Fudan University, Shanghai 200032, China
Correspondence to: Dr. Jiang Lin, Department of Radiology, Affiliated Zhongshan Hospital, Fudan University, Shanghai 200032, China. linjiang@zshospital.net
Telephone: +86-21-64041990 Ext 2463 **Fax:** +86-21-64038472
Received: 2003-04-02 **Accepted:** 2003-05-11

Abstract

AIM: To evaluate the role of three-dimensional contrast-enhanced magnetic resonance angiography (3D CE MRA) in the diagnosis of Budd-Chiari syndrome (BCS).

METHODS: Twenty-three patients with BCS underwent 3D CE MRA examination, in which 13 cases were secondary to either hepatocellular carcinoma (11 cases), right adrenal carcinoma (1 case) or thrombophlebitis (1 case) and 10 suffered from primary BCS. The patency of the inferior vena cava (IVC), hepatic and portal veins as well as the presence of intra- and extrahepatic collaterals, liver parenchymal abnormalities and porto-systemic varices were evaluated. Inferior vena cavography was performed in 10 cases. The diagnosis of IVC obstruction by 3D CE MRA was compared with that demonstrated by inferior vena cavography.

RESULTS: The major features of BCS could be clearly displayed on 3D CE MRA. Positive hepatic venous signs included tumor thrombosis (9 cases), tumor compression (2 cases), nonvisualization (4 cases) and focal stenosis (2 cases). Positive IVC findings were noted as severe stenosis or occlusion (10 cases), tumor invasion (2 cases), thrombosis (3 cases), thrombophlebitis (1 case) and septum formation (3 cases). Intrahepatic collaterals were shown in 9 patients, 2 of them with "spider web" sign. The displayed extrahepatic collaterals included dilated azygos and hemi-azygos veins (13 cases) and left renal-inferior phrenic-pericardiophrenic veins (2 cases). The occlusion of the left intrahepatic portal veins was found in 2 cases. Porto-systemic varices were detected in 10 patients. Liver parenchymal abnormalities displayed by 3D CE MRA were enlargement of the caudate lobe (7 cases), heterogenous enhancement (18 cases) and complicated tumors (13 cases). Compared with the inferior vena cavography performed in 10 cases, the accuracy of 3D CE MRA was 100 % in the diagnosis of IVC obstruction.

CONCLUSION: 3D CE MRA can display the major features of BCS and provide an accurate diagnosis.

Lin J, Chen XH, Zhou KR, Chen ZW, Wang JH, Yan ZP, Wang P. Budd-Chiari syndrome: Diagnosis with three-dimensional contrast-enhanced magnetic resonance angiography. *World J Gastroenterol* 2003; 9(10):2317-2321
http://www.wjgnet.com/1007-9327/9/2317.asp

INTRODUCTION

Budd-Chiari syndrome (BCS) is a rare disease caused by the obstruction of the hepatic venous outflow or the inferior vena cava (IVC) above the hepatic vein[1]. It often occurs secondary to intrinsic vascular thrombosis, hepatic tumor invasion/compression, or associates with an idiopathic obstructing membrane[1,2]. The clinical signs of ascites, abdominal pain and hepatomegaly are the typical triad of BCS. Since these signs are nonspecific, the clinical diagnosis of this syndrome is difficult. Conventionally, X-ray angiography and/or liver biopsy are used to confirm the diagnosis of BCS with the limitation of invasiveness. Ultrasound (US), computed tomography (CT) and magnetic resonance imaging (MRI) are the noninvasive imaging techniques currently used in the evaluation of the patency of hepatic veins, IVC and portal vein. However, some limitations are also existed in each of these modalities[2-7].

Three-dimensional contrast-enhanced magnetic resonance angiography (3D CE MRA) is a new technique and widely used in the imaging of the arterial system, portal venous system and central venous system[8-16]. However, to our knowledge, few studies have been reported so far concerning its use in the diagnosis of BCS[17]. Therefore, this study was conducted to evaluate the usefulness of this technique in the imaging of BCS and to present various findings of BCS demonstrated on 3D CE MRA.

MATERIALS AND METHODS

Patients

Twenty-three patients with BCS underwent 3D CE MRA. There were 20 men and 3 women ranging from 26 to 56 years of age (average age 38 years). In 11 patients, BCS was secondary to the invasion and occlusion of the hepatic vein and/or IVC by hepatocellular carcinoma (HCC). In 1 patient, BCS was resulted from tumor invasion of IVC by right adrenal carcinoma. In 1 patient, IVC obstruction was due to superior extension of pelvic thrombophlebitis. The above 13 patients were considered to be secondary BCS. Ten patients had primary BCS with an unknown origin. The diagnosis of BCS was confirmed by inferior vena cavography in 10 cases, percutaneous liver biopsy in 2 cases, and surgery in 5 cases. The diagnosis of the remaining 6 cases was confirmed by combined color Doppler sonography and contrast-enhanced CT.

3D CE MRA examination

All scans were performed using a 1.5T MR imager (Signa, General Electric Medical Systems, Milwaukee, WI.) and a body coil. After the localizing images were obtained, a breathhold T1-weighted fast multiplanar spoiled gradient-echo (FMPSPGR) sequence (repetition time/echo time, 150/4.2 msec; flip angle, 90°; field of view, 360 mm; matrix, 128×256; 18 slices; slice thickness, 7.0 mm; gap, 3.0 mm; one signal acquired) and a respiratory-triggered T2-weighted fast spin-echo sequence (repetition time/echo time, 2800-4200/80 msec; echo train length 8-12, field of view, 360 mm; matrix, 128×256; 18 slices; slice thickness, 7.0 mm; gap, 3.0 mm; 2 signals

acquired) were performed in the liver. For 3D CE MRA, a breath-hold 3D fast spoiled gradient-echo sequence (repetition time/echo time, 5.2-10.2/1.2-1.9 msec; flip angle, 30° or 45°; field of view, 360-480 mm; matrix, 128×256; imaging volume, 75-168 mm; number of partitions, 24-30; one signal acquired; and acquisition time, 19-28 sec) was used.

With T1-weighted and T2-weighted images as reference, the imaging volume of 3D CE MRA was acquired in a coronal plane to cover the hepatic veins, IVC, portal veins and collateral vessels. The imaging volume was determined by a radiologist depending on each patient´s abnormalities, liver size and ability of breathholding.

A gadolinium chelate called gadopentetate-dimeglumine (Magnevist; Schering AG, Berlin, Germany) was used as a contrast material for all examinations, with a concentration of 0.15 mmol per kilogram of body weight. In all cases the contrast material was injected by an experienced MR technician through an antecubital vein with an injection rate of approximately 3 ml/sec. In 2 patients, however, due to poor visualization of IVC after injection of the contrast material into an arm vein, the study was repeated and the contrast agent was injected via a pedal vein for assessment of IVC. Scanning was commenced immediately after the injection and repeated three times with a 6-second delay between each acquisition for patient' s breathing. The first acquisition was the imaging of the arterial phase, the second acquisition was the portal venous phase for demonstration of the portal vein and IVC, while the third acquisition coincided with the image of the late venous phase for visualization of the hepatic veins. Source images of each acquisition were reviewed first, and then these images were reconstructed on a workstation (Advantage windows workstation, General Electric Medical Systems, Milwaukee, WI) to produce projectional images like X-ray angiography. Both maximum intensity projection (MIP) and multiplanar reconstruction (MPR) techniques were employed to analyze the acquired image.

Image analysis

3D CE MRA images were reviewed together by two radiologists unaware of the patients' clinical statuses and other imaging findings. The patency of the hepatic veins, IVC and portal veins was assessed. The presence of intra- and extrahepatic collaterals, liver parenchymal abnormalities and porto-systemic varices were also noted. Inferior vena cavography was performed in 10 cases. The diagnosis of IVC obstruction by 3D CE MRA was compared with that demonstrated by inferior vena cavography.

RESULTS

3D CE MRA findings

Hepatic veins 3D CE MRA demonstrated tumor thrombosis of two or three hepatic veins in each of the 9 patients with HCC (Figure 1). The right and middle hepatic veins were severely compressed and distorted by HCC in 2 patients. Nonvisualization of hepatic veins occurred in 4 patients with primary BCS. Focal stenosis of the right and middle hepatic veins near the caval confluence was detected in 2 patients with primary BCS (Figure 2).

IVC Severe stenosis or occlusion of the IVC was found in 10 patients (Figure 3), 3 of them were associated with the external compression or direct invasion of IVC by HCC. Tumor thrombosis was found in 3 cases with HCC (Figure 1). Direct invasion of IVC by right adrenal tumor was observed in 1 case. Thrombosis of IVC was shown in 1 patient with pelvic thrombophlebitis. A septum or obstructing membrane was demonstrated in the IVC in 3 patients (Figure 4). Localized dilatation of the distal IVC and renal veins were shown in 2 cases with IVC obstruction. In 10 patients with inferior vena cavography, the site and extent of IVC obstruction and distribution of collaterals presented by 3D CE MRA were in agreement with those by cavography (Figure 3). The accuracy of 3D CE MRA was 100 % in the diagnosis of IVC obstruction.

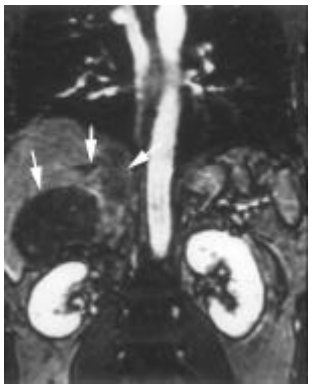

Figure 1 Source image of three-dimensional contrast-enhanced magnetic resonance angiography shows tumor thrombosis of the right hepatic vein (short arrow) and inferior vena cava (long arrow). A hypointense hepatocellular carcinoma (arrowhead) is shown simultaneously.

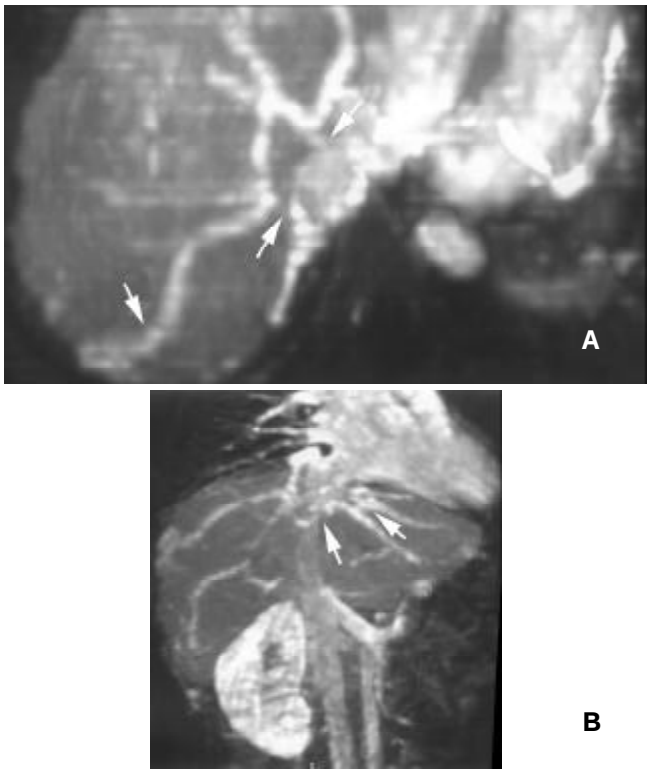

Figure 2 A: Axial reconstruction of three-dimensional contrast-enhanced magnetic resonance angiography demonstrates focal stenosis of right and middle hepatic veins (arrow heads). Intrahepatic collateral between right hepatic vein and subcapsular vein is also demonstrated (arrow). B: Coronal reconstruction reveals fine collaterals between hepatic veins (arrows), resembling a "spider web".

Intra-and extrahepatic collaterals 3D CE MRA revealed fine venous collaterals between the right hepatic veins and subcapsular veins, and between the right, middle and left hepatic veins in 2 patients with focal hepatic vein stenosis, appearing as the typical "spider web" sign (Figure 2B). Large and tortuous veins between enlarged right inferior accessory hepatic veins and right main hepatic veins were identified in 3

patients with IVC occlusion (Figure 3B). Various extrahepatic collaterals were found in the abdominal wall, peritoneal and retroperitoneal areas. Prominent azygos and hemiazygos veins were demonstrated in 13 patients. The left renal-inferior phrenic-pericardiophrenic collaterals were displayed in 2 patients (Figure 5).

Portal veins and porto-systemic varices The portal veins were found patent in all observed patients except 2 whose left intrahepatic portal veins were occluded (Figure 6). Gastroesophageal/esophageal varices and spontaneous splenorenal shunts were identified in 8 and 2 patients respectively.

Liver parenchyma An enlarged caudate lobe was found in 7 patients. Heterogenous liver enhancement was observed in 18 cases (Figure 6). HCC, which showed hyperintensity in arterial phase and hypointensity in portal venous phase, was found in 13 patients (Figure 1). In 2 of them, the tumor was developed after the primary BCS formation, because these two patients underwent long-term follow-up studies and the initial imaging findings indicated no intrahepatic tumors.

Figure 3 A: Source image depicts occlusion of the inferior vena cava(arrowhead). B: Maximum intensity projection of three-dimensional contrast-enhanced magnetic resonance angiography depicts tortuous intrahepatic collaterals (arrows) between right inferior accessory hepatic vein and right main hepatic vein. C: Inferior vena cavography confirms the occlusion of the inferior vena cava (arrowhead) and the intrahepatic collaterals (arrow).

Figure 4 Three-dimensional contrast-enhanced magnetic resonance angiography identifies a septum (arrowheads) in the inferior vena cava.

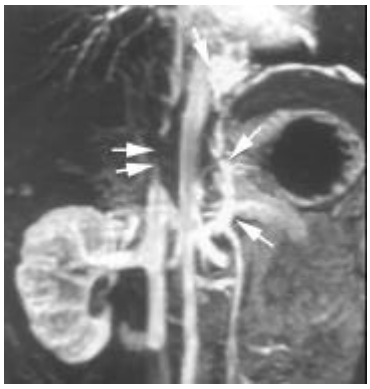

Figure 5 Three-dimensional contrast-enhanced magnetic resonance angiography detects occlusion of the inferior vena cava(white arrowheads), prominent left renal-inferior phrenic-pericardiophrenic collaterals (arrows) and esophageal varix (black arrowhead).

Figure 6 Three-dimensional contrast-enhanced magnetic resonance angiography demonstrates occlusion of the left portal vein (arrowhead) and heterogeneous enhancement pattern of the liver (arrows).

DISCUSSION

BCS is difficult to be diagnosed clinically. However, accurate and early diagnosis is important for its treatment. Radiologic assessment is an important step for its diagnosis. Diagnosis by US was noninvasive, relatively inexpensive and readily available, but its accuracy was limited by operator' s experience, poor acoustic window, inaccessible anatomic structure and body forms[1,3,7]. Contrast-enhanced CT was readily available too, but it used ionizing radiation and required intravenous administration of a large amount of iodinated contrast material with the risk of

nephrotoxicity and possible allergic reactions[1,5,6]. X-ray angiography was the reference criteria for the evaluation of BCS, due to its superb spatial resolution[1,3], but it was invasive and uncomfortable. Like CT, it also involved radiation and use of iodinated contrast material. Disadvantages also included high cost, requirement of operator' s expertise (especially for hepatic venography), and associated complications such as hemorrhage. MRI and non-enhanced magnetic resonance angiography (MRA) with time-of-flight (TOF) and phase-contrast (PC) techniques were other non-invasive means for demonstrating the hepatic venous system, but were limited by long acquisition time, motion and flow artifacts, and saturation effects[2,4,18-21].

3D CE MRA is a recently developed, non-invasive, fast and easy to be performed technique, which is capable of depicting vascular anatomy in multiple projections. It involves no radiation. With this technique, the imaging of the hepatic veins, IVC and portal veins is accomplished with only one injection of contrast material and short breath holding. It requires only a peripheral venous injection of a small amount of gadolinium, which is much safer than iodine-based contrast material. By using gadolinium to shorten the T1 value of the blood, it overcomes flow artifacts and saturation effects in TOF and PC. Moreover, it permits assessment of liver parenchyma and extravascular abnormalities during investigation of the vascular system[12,15,17]. So 3D CE MRA has many advantages over the currently more conventional methods for imaging the BCS.

According to our study, 3D CE MRA was able to demonstrate the patency of the hepatic veins, IVC and portal veins. It could show intra- and extrahepatic collaterals as well as porto-systemic varices caused by cirrhosis. 3D CE MRA could distinguish extravascular compression from intravascular thrombosis, detect liver abnormalities and evaluate the extent of the disease. By means of only one examination, 3D CE MRA provided all these crucial information for accurate diagnosis of BCS and for possible surgical or interventional managements, such as porto-caval shunt, liver transplantation, transjugular intrahepatic porto-systemic shunt (TIPSS), percutaneous transluminal angioplasty (PTA) and stent placement[22-27].

Among 13 patients of secondary BCS, tumor thrombosis, external compression and direct invasion of hepatic veins and/or IVC by tumors were the main causes of this disease. Through demonstration of intra- and extrahepatic disorders and the involved blood vessels, 3D CE MRA could disclose the etiology of BCS. For patients with primary BCS, nonvisualization, focal stenosis of the hepatic veins, occlusion or a septum formed in IVC were the most common findings on 3D CE MRA, as have been reported by Miller *et al*[5] with CT and MRI techniques. Compared with vena cavography, 3D CE MRA was 100 % accurate in diagnosis of IVC obstruction. On the basis of this study and Erden' s report[17], 3D CE MRA could replace inferior vena cavography for diagnosing IVC obstruction.

3D CE MRA could evaluate the intra- and extrahepatic collateral pathways. Identification of intrahepatic collateral veins is highly suggestive of BCS[6,17,28]. The intrahepatic collateral veins divert blood away from the stenotic or occluded hepatic vein and into a patent hepatic vein or a systemic vein. According to Cho' s report[6], intrahepatic collaterals were poorly defined on contrast-enhanced CT. In this study, 3D CE MRA found these collateral veins in 2 patients with stenosis of the hepatic veins. On 3D CE MRA, they were identified either by typical "spider web" sign or by large connecting veins between accessory and main hepatic veins. The dilated azygos and hemiazygos veins were the most commonly collateralized extrahepatic routes shown in this study. The infrequent left renal-inferior phrenic-pericardiophrenic collaterals were also seen on 3D CE MRA.

Our study indicated that a strong point of 3D CE MRA was to display the portal venous system simultaneously with hepatic veins and IVC. Obstruction or increased pressure in hepatic veins resulted in portal hypertension and portal flow stasis, which might further cause porto-systemic varices and portal vein thrombosis. Complications of portal hypertension were fatal in more than 50 % of BCS patients[27]. Thus the accurate delineation of the abnormalities of the portal vein, and the anatomic relationship between portal vein, hepatic veins and IVC were very important, particularly when preparing the treatment with porto-caval shunt or TIPSS[22-24,27]. In this study, 3D CE MRA showed the ability to provide all these relevant information.

Hypertrophy of the caudate lobe was found on 3D CE MRA. This was related to independent blood supply and drainage of this lobe. Heterogeneous enhancement pattern observed by 3D CE MRA has been already known from studies on contrast-enhanced CT[1]. It reflected the hemodynamic disturbance in the liver with BCS. 3D CE MRA found 2 patients with primary BCS developed HCC during a long-term follow-up period. The development of HCC in patients with chronic BCS has been reported in the literature[29]. According to that report, many factors, such as chronic viral infection or cirrhosis might play a role in the development of this malignancy.

Our study had two limitations. Firstly, a detailed comparison between 3D CE MRA and X-ray angiography was not performed, because none of our patients underwent hepatic venography and only some had inferior vena cavography. But 3D CE MRA could demonstrate various findings of BCS, which might provide clues to the correct diagnosis. Secondly, the opacification of IVC, after injection of contrast material into an arm vein, was inadequate in 2 patients with severe cirrhosis, portal hypertension and edema. We speculated this was due to the dilution of the contrast material in the porto-systemic collaterals, enlarged spleens and increased extracellular fluid. In these circumstances, the IVC could be enhanced properly by injecting contrast material into a pedal vein.

In conclusion, 3D CE MRA can display various features of BCS and provide an accurate diagnosis.

REFERENCES

1 **Stanley P**. Budd-Chiari syndrome. *Radiology* 1989; **170**(3Pt 1): 625-627

2 **Kane R**, Eustace S. Diagnosis of Budd-Chiari syndrome: comparison between sonography and MR angiography. *Radiology* 1995; **195**: 117-121

3 **Millener P**, Grant EG, Rose S, Duerinckx A, Schiller VL, Tessler FN, Perrella RR, Ragavendra N. Color Doppler imaging findings in patients with Budd-Chiari syndrome: correlation with venographic findings. *Am J Roentgenol* 1993; **161**: 307-312

4 **Soyer P**, Rabenandrasana A, Barge J, Laissy JP, Zeitoun G, Hay JM, Levesque M. MRI of Budd-Chiari syndrome. *Abdom Imaging* 1994; **19**: 325-329

5 **Miller WJ**, Federle MP, Straub WH, Davis PL. Budd-Chiari syndrome: imaging with pathologic correlation. *Abdom Imaging* 1993; **18**: 329-335

6 **Cho OK**, Koo JH, Kim YS, Rhim HC, Koh BH, Seo HS. Collateral pathways in Budd-Chiari syndrome: CT and venographic correlation. *Am J Roentgenol* 1996; **167**: 1163-1167

7 **Ralls PW**, Johnson MB, Radin DR, Boswell WD Jr, Lee KP, Halls JM. Budd-Chiari syndrome: detection with color Doppler sonography. *Am J Roentgenol* 1992; **159**: 113-116

8 **Leung DA**, Mckinnon GC, Davis CP, Pfammater T, Krestin GP, Debatin JF. Breath-hold, contrast-enhanced, three-dimensional MR angiography. *Radiology* 1996; **200**: 569-571

9 **Kopka L**, Rodenwaldt J, Vosshenrich R, Fischer U, Renner B, Lorf T, Graessner J, Ringe B, Grabbe E. Hepatic blood supply: comparison of optimized dual phase contrast-enhanced three-dimen-

sional MR angiography and digital subtraction angiography. *Radiology* 1999; **211**: 51-58
10 **Zeh H**, Choyke PL, Alexander HR, Bartlett D, Libutti SK, Chang R, Summers RM. Gadolinium-enhanced 3D MRA prior to isolated hepatic perfusion for metastases. *J Comput Assist Tomogr* 1999; **23**: 664-669
11 **Glockner JF**, Forauer AR, Solomon H, Varma CR, Perman WH. Three-dimensional gadolinium-enhanced MR angiography of vascular complications after liver transplantation. *Am J Roentgenol* 2000; **174**: 1447-1453
12 **Hawighorst H**, Schoenberg SO, Knopp MV, Essig M, Miltner P, van Kaick G. Hepatic lesions: morphologic and functional characterization with multiphase breath-hold 3D gadolinium-enhanced MR angiography-initial results. *Radiology* 1999; **210**: 89-96
13 **Saddik D**, Frazer C, Robins P, Reed W, Davis S. Gadolinium-enhanced three-dimensional MR portal venography. *Am J Roentgenol* 1999; **172**: 413-417
14 **Laissy JP**, Trillaud H, Douek P. MR angiography: noninvasive vascular imaging of the abdomen. *Abdom Imaging* 2002; **27**: 488-506
15 **Thornton MJ**, Ryan R, Varghese JC, Farrell MA, Lucey B, Lee MJ. A three-dimensional gadolinium-enhanced MR venography technique for imaging central veins. *Am J Roentgenol* 1999; **173**: 999-1003
16 **Shinde TS**, Lee VS, Rofsky NM, Krinsky GA, Weinreb JC. Three-dimensional gadolinium-enhanced MR venographic evaluation of patency of central veins in the throrax: initial experience. *Radiology* 1999; **213**: 555-560
17 **Erden A**, Erden I, Krayalcin S, Yurdaydin C. Budd-Chiari syndrome: evaluation with multiphase contrast-enhanced three-dimensional MR angiography. *Am J Roentgenol* 2002; **179**: 1287-1292
18 **Colletti PM**, Christopher TO, Terk MR, Boswell MD. Magnetic resonance of the inferior vena cava. *Magn reson imaging* 1992; **10**: 177-185
19 **Ruehm SG**. MR venography. *Eur Radiol* 2003; **13**: 229-230
20 **Butty S**, Hagspiel KD, Leung DA, Angle JF, Spinosa DJ, Matsumoto AH. Body MR venography. *Radiol Clin North Am* 2002; **40**: 899-919
21 **Mohiaddin RH**, Wann SL, Underwood R, Firmin DN, Rees S, Longmore DB. Vena caval flow: assessment with cine MR velocity mapping. *Radiology* 1990; **177**: 537-541
22 **Slakey DP**, Klein AS, Venbrux AC, Cameron JL. Budd-Chiari syndrome: current management options. *Ann Surg* 2001; **233**: 522-527
23 **Perello A**, Garcia-Pagan JC, Gilabert R, Suarez Y, Moitinho E, Cervantes F, Reverter JC, Escorsell A, Bosch J, Rodes J. TIPS is a useful long-term derivative therapy for patients with Budd-Chiari syndrome uncontrolled by medical therapy. *Hepatology* 2002; **35**: 132-139
24 **Schepke M**, Sauerbruch T. Transjugular portosystemic stent shunt in treatment of liver diseasse. *World J Gastroenterol* 2001; **7**: 170-174
25 **Pelage JP**, Denys A, Valla D, Sibert A, Sauvanet A, Belghiti J, Menu Y. Budd-Chiari syndrome due to prothrombotic disorder: mid-term patency and efficacy of endovascular stents. *Eur Radiol* 2003; **13**: 286-293
26 **Suhocki PV**, Trotter JF. Percutaneous hepatic vein reconstruction for Budd-Chiari syndrome. *Am J Roentgenol* 1998; **171**: 189-191
27 **Blum U**, Rossle M, Haag K, Ochs A, Blum HE, Hauenstein KH, Astinet F, Langer M. Budd-Chiari syndrome: technical, hemodynamic, and clinical results of treatment with transjugular intrahepatic portosystemic shunt. *Radiology* 1995; **197**: 805-811
28 **Naganuma H**, Ishida H, Konno K, Komatsuda T, Hamashima Y, Ishida J, Masamune O. Intrahepatic venous collaterals. *Abdom Imaging* 1998; **23**: 166-171
29 **Vilgrain V**, Lewin M, Vons C, Denys A, Valla D, Flejou JF, Belghiti J, Menu Y. Hepatic nodules in Budd-Chiari syndrome: imaging features. *Radiology* 1999; **210**: 443-450

Edited by Zhu L